

# Wave functions in the Critical Phase: a Planar *Sierpiński* Fractal Lattice

Qi Yao<sup>1,2,\*</sup>, Xiaotian Yang<sup>3,\*</sup>, Askar A. Iliasov<sup>4</sup>, Mikhail I. Katsnelson<sup>5</sup>, and Shengjun Yuan<sup>3,6,†</sup>

<sup>1</sup>Quantum Science Center of Guangdong-Hong Kong-Macao Greater Bay Area (Guangdong), Shenzhen 518045, China

<sup>2</sup>Institute of Quantum Precision Measurement, State Key Laboratory of Radio Frequency Heterogeneous Integration, College of Physics and Optoelectronic Engineering, Shenzhen University, Shenzhen 518060, China

<sup>3</sup>Key Laboratory of Artificial Micro- and Nano-structures of Ministry of Education and School of Physics and Technology, Wuhan University, Wuhan, Hubei 430072, China

<sup>4</sup>Department of Physics, University of Zurich, Winterthurerstrasse 190, 8057 Zurich, Switzerland

<sup>5</sup>Institute for Molecules and Materials, Radboud University, Heijendaalseweg 135, 6525 AJ Nijmegen, The Netherlands

<sup>6</sup>Wuhan Institute of Quantum Technology, Wuhan 430206, China

(Dated: June 25, 2024)

Electronic states play a crucial role in many quantum systems of moire superlattices, quasicrystals, and fractals. As recently reported in *Sierpiński* lattices [Phys. Rev. B 107, 115424 (2023)], the critical states are revealed by the energy level-correlation spectra, which are caused by the interplay between aperiodicity and determined self-similarity characters. In the case of the *Sierpiński Carpet*, our results further demonstrate that there is some degree of spatial overlap between these electronic states. These states could be strongly affected by its ‘seed lattice’ of the *generator*, and slightly modulated by the dilation pattern and the geometrical self-similarity level. These electronic states are multifractal by scaling the  $q$ -order inverse participation ratio or fractal dimension, which correlates with the subdiffusion behavior. In the *gene* pattern, the averaged state-based multifractal dimension of second-order would increase as its *Hausdorff dimension* increases. Our findings could potentially contribute to understanding quantum transports and single-particle quantum dynamics in fractals.

## I. INTRODUCTION

Translational invariance of atomic arrangement in crystals leads to the band theory based on the Bloch theorem; Bloch character of electronic wave functions describes enormous amount of properties of crystalline solids [1–5]. This symmetry is absent in randomly disordered systems [6–8] as well as in incommensurate (quasiperiodic) systems such as 1D Fibonacci chain [9], 2D Penrose tiling [10, 11], Ammann-Beenker lattice [12, 13]), and hierarchical tiling of *Sierpiński* lattices [14–16] and Koch fractals [17]. In all these cases the tools dramatically different from the band theory are required. In particular, the concept of Anderson localization [18] is necessary to understand the properties of disordered systems [6–8]. After many years of efforts, we have well developed mathematical tools to describe this and related phenomena [19], and some of these tools will be named below. The cases of regular but not translationally invariant systems such as quasicrystals and fractals are much less studied, and we are still far from more or less complete understanding of their electron properties.

To better study these aperiodic structures, many researchers have developed various alternative theoretical methods, including renormalization group technique [20–28], transfer matrix [29–32], level-spectra statistics [33] from random matrices theory [34, 35], one-parameter scaling based on studies of correlated length for coherent

structures at different size [36, 37] or localized length [38] in Anderson model [18, 39], the state-based multifractality scaling [32], studies of transport properties [40–42] etc.

Following the above timeline, two key objects, namely energy spectra [33–35] and wave functions in real space [36, 37], come in view, which can be exploited to analyze electronic [43–45] and phonon [46] systems. For instance, the wave functions belong to one of three types: the characteristically (Bloch) extended state [4] in periodicity-translation crystals; the typically localized state [18] in disorder-induced systems by impurities, defects, etc; or the state behaves in between and remains critical in several quasicrystals likely Fibonacci chain [47], Thue-Morse lattice [48] or some Penrose tiling [49]. In general, these could be distinguished as follows: whereas the localized wave functions have exponentially localized envelope with  $|\psi(r)| \sim \exp(-\alpha r^\beta)$ , where  $\alpha$  and  $\beta$  are the spatial parameters, the decay of the critical states following the power-law form with  $|\psi(r)| \sim |r|^{-\alpha}$  (or more complicated envelope, e.g., the localized edge states in ring shape [43] and critical states with the SKK form in Penrose lattices [44]), respectively. Note that *in the absence of disorder*, lattice frustration possibly induces the fragmented states (i.e., critical states) in quasicrystals and fractals, these states also become more complex with various long-range orders.

*Sierpiński Carpet*  $SC(n, m, g^*)$  as a class of fractals [14, 50–53], where  $(n, m)$  is the parameters of the *generator*  $(n, m)$  and the geometrical hierarchy level  $g^*$ , it resembles a periodic square lattice in 2D, whose order of ramification is infinite. Experimentally, these fractal objects can be accessed by arranging waveguide tube [54]

\* These authors contributed equally to this work.

† Corresponding author: [s.yuan@whu.edu.cn](mailto:s.yuan@whu.edu.cn)

and electric circuit [55] or printing acoustic lattices [56] in desired fractal shapes [14, 57]. In Ref. [58], when a single electron roams upon the  $SC(n, m, g^*)$  lattices, we have found that all electronic states reside in the critical phase, which isolates that near mobility edge where Anderson transition occurs [39]. This trait affects their observable properties of quantum conductance [59] and QC-based box-counting dimension, plasmas [60], and Hall conductance [61], among others.

To obtain more insight into fractal lattices, we would focus on probing the spatial envelope of electronic states, rather than the nearest energy-correlation spectra. And two aspects are studied: (i) the state envelope in these  $SC(n, m, g^*)$  lattices at various energy bands; (ii) how other factors, such as the *generator*( $n, m$ ), dilation pattern, fractal dimension  $\mathcal{D}_H$ , and geometrical hierarchy level  $g^*$ , affect the critical states (CSs)? It is potentially crucial for further investigating the disorder-induced localization [62] or many-body correlation effect [63] in *Sierpiński* fractal lattices.

The rest of the paper is organized as follows. In Sec. II, we introduce the single-electron gas model on the  $SC(n, m, g^*)$  lattices and the state-based multifractality analysis. Our results are presented in Sec. III. Under three lattice-dilation patterns with  $SC(n, m, 3)$  lattices, the electronic states are sketched by their density profile in Sec. III A, and whose multifractal properties are shown in Sec. III B. A conclusion is reached in Sec. IV.

## II. LATTICE, MODEL, AND METHOD

*Fractal lattices and model.*— First, we retrospect the fractal  $SC(n, m, g^*)$  lattices that we denoted previously, see Fig. 1 in Ref. [58]. Using the *generaotr*( $n, m$ ) and two illustrations of the *self* and *gene* patterns ( $M_{se}$  and  $M_{ge}$ ), various  $SC(n, m, g^*)$  lattices are dilated. Here, these two patterns are our main interest, adding the *vari* pattern as a comparison, which is a variation of the *self* pattern. Second, a noninteracting electron gas is confined in the  $SC(n, m, g^*)$  lattices, which is modeled by

$$H = -t \sum_{\langle i, j \rangle} (\mathbf{c}_i^\dagger \mathbf{c}_j + \mathbf{c}_j^\dagger \mathbf{c}_i) + V \sum_i f(i) \mathbf{c}_i^\dagger \mathbf{c}_i. \quad (1)$$

The first term describes a single electron hops between the nearest neighbor site pair  $\langle i, j \rangle$ . Setting the strength  $t$  as the energy unit. The on-site potential with strength of  $V$  includes in the second term, which is tailored locally by the function  $f(i)$  in Anderson [18], Harper [64], Aubry or Aubry-André [65], and Aubry-André-Harper model [65, 66]. Third, for consistency with Ref. [58], and only taking the lattice topology effect into account, we set up  $V = 0$ . The results of the level-spectra statistics indicate that the electronic states might be intermediately critical (in other words, they always partially occupy the entire lattice, or the tail of the level-correlation spectra follows the power-law trait). We further use the new tool to quantify these electronic states.

*State-based multifractality analysis.*— For arbitrary state  $\psi$ , measuring its spatial extension in lattice, as a convenient tactic, can reveal some inherent traits, which is exploited in studying the localization problem with several concepts such as localization length [67, 68], structural entropy [69, 70], participation ratio [70], and multifractality [32]. We adopt the  $2q$ -norm multifractality [32] by the given formula,

$$\chi_q(\psi, \Omega) = \frac{\sum_{i \in \mathcal{R}} |\psi(i)|^{2q}}{\left(\sum_{i \in \mathcal{R}} |\psi(i)|^2\right)^q}, \quad (2)$$

with  $q$ -order inverse participation ratio (IPR)  $\chi_q(\psi, \Omega)$ , where  $\Omega$  is the number of site counted in region  $\mathcal{R}$ .

To understand Eq. 2 well, we take three examples: i) one of wave function is evenly extended in the spatial lattice, i.e.  $\psi(r) = \text{const}$ , then we have  $\chi_q(\psi, \Omega) = \Omega^{1-q}$  with the lattice size  $\Omega$ ; ii) assuming  $\psi(r)$  have the power-law-decay envelope with an exponent  $\alpha$ , instead

$$\chi_q(\psi, \Omega) \simeq \begin{cases} \Omega^{-2(q-1)} & (0 \leq \alpha < 1/q) \\ \Omega^{-2q(1-\alpha)} & (1/q \leq \alpha < 1), \text{ for } q > 1. \\ \Omega^0 & (1 \leq \alpha); \end{cases} \quad (3)$$

iii) another one has the envelope of exponential decaying and an oscillation tail, namely the localized state. If the third state continues to degenerate highly and only occupies several sites, we refer to it as the confined state. One might imagine the single-site-occupied state, obviously having  $\chi_q(\psi, \mathcal{R}) = 1$ . Note that  $\chi_q(\psi, \mathcal{R})$  depends obviously on the region  $\Omega(\mathcal{R})$  one computes. Because different states are associated with lattices of various sizes, it becomes tricky to compare these electronic states directly.

However, using  $\mathcal{D}_q^\psi(\psi)$  could avoid this issue. Since the quantity  $\chi_q(\psi, \mathcal{R})$  scales exponentially as  $\mathcal{R}^{-(q-1)\mathcal{D}_q^\psi(\psi)}$ , which is linked the  $q$ -th fractal dimension [71],

$$\mathcal{D}_q^\psi(\psi) = \lim_{\mathcal{R} \rightarrow \infty} \frac{-1}{q-1} \frac{\log \chi_q(\psi(i), \mathcal{R})}{\log \Omega(\mathcal{R})}. \quad (4)$$

In general, the second-order quantities of  $q = 2$  demarcate the extended (localized) state with  $\chi_2(\psi) = \Omega^{-1}$  and  $\mathcal{D}_2^\psi(\psi) = 1$  ( $\chi_2(\psi) \simeq 1$  and  $\mathcal{D}_2^\psi(\psi) \simeq 0$ ). There is a special situation where our observed values are just in between, leading the system to a critical state. It can happen in two scenarios. One is near the mobility edge when Anderson transition occurs [72, 73], The other scenario is found in quasicrystals [32], where geometric frustration plays a role. In both cases, the electronic states are spatially fragmented differently.

Our work mainly explores the CSs within fractals. It is interesting to note that when two CSs are close in characteristics, we can spot the differences between them by measuring the IPR  $\chi_q(\psi, \mathcal{R})$  and the state-based fractal dimension  $\mathcal{D}_q^\psi(\psi)$ , especially when using a higher value of  $q$ . This aspect becomes crucial when we observe the vast clustering of CSs in the spectra of  $\mathcal{D}_q^\psi(\psi)$ .

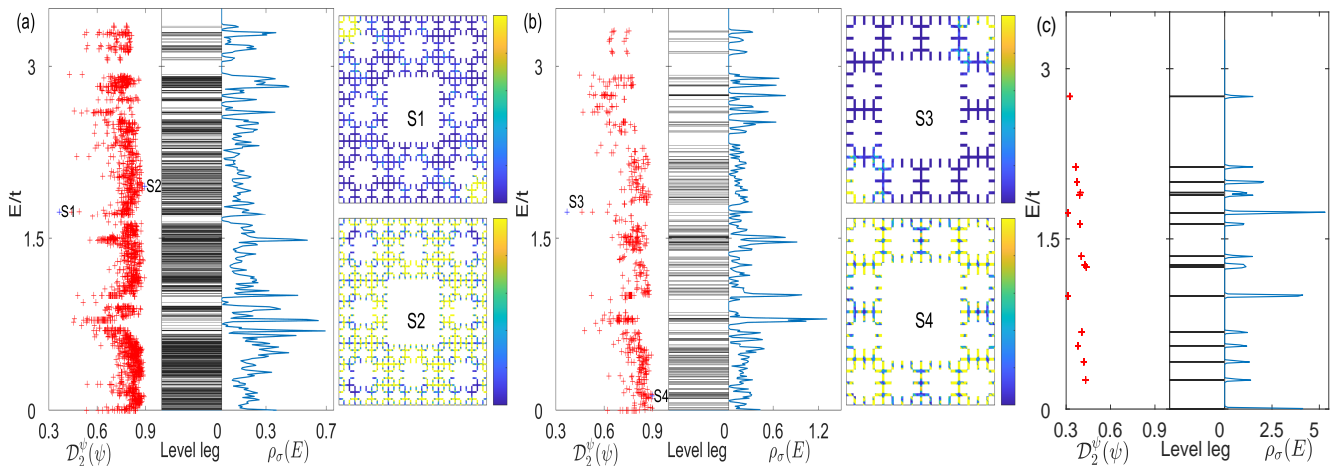


FIG. 1. (Color online) Schematic illustration of the  $SC(n, m, g^*)$  fractal lattices by a paradigmatic  $generator(4, 2)$  under the *self* (a), *gene* (b), and auxiliary *vari* pattern (c), respectively. Geometrical hierarchy level  $g^* = 3$ . Energy spectra are symmetric about  $E = 0$ ; hence, the upper half panel is considered, i.e.,  $0 \leq E \leq 4t$ . At left subpanel in (a), (b), and (c), fractal dimension  $\mathcal{D}_2^\psi(\psi)$  (red cross dot) of wave function measures its degree of spatial extension in the whole lattice; level leg  $E$  (black line in middle subpanel) and DoS  $\rho_\sigma(E)$  (blue curve) with a blurred energy width  $\sigma = 0.0056t$  [74] in right subpanel. Two extreme (minimum and maximum) cases of  $\mathcal{D}_2^\psi(\psi)$  give four states, which are marked in blue with  $S1$  and  $S3$  ( $S2$  and  $S4$ ) in the upper (bottom) subfigure. The scaled probability density  $Ar|\psi_{E_n}(i)|^2$  maps into a colorbar region from 0 to  $Ar$ .

### III. RESULTS AND DISCUSSION

In this section, we would study the critical states from different perspectives. These include: i) examining their density profile, which helps us understand how the wave function occupies the entire fractal lattice, akin to analyzing the IPR; ii) investigating the multifractality scaling (fractal dimension), which is related to the subdiffusion behaviors, and could be observed by the dynamical evolutions in larger fractals.

#### A. The density profile on three $SC(n, m, 3)$ lattices

To highlight how the CSs in fractal lattices are distinct from the other two types of states—extended and localized—we start by examining their spatial density profiles. We demonstrate this using three examples of  $SC(4, 2, g^* = 3)$  lattices. These lattices are designed sequentially following specific patterns: the *self* pattern with a matrix  $M_{se} = [1 \ 1 \ 1; 1 \ 0 \ 1; 1 \ 1 \ 1]$ , the *gene* pattern with  $M_{ge}(1) = [1 \ 1 \ 1 \ 1; 1 \ 0 \ 0 \ 1; 1 \ 0 \ 0 \ 1; 1 \ 1 \ 1 \ 1]$ , and the *vari* pattern, a variation of the ‘self’ pattern, with  $M_{va} = [1 \ 0 \ 0; 0 \ 0 \ 1; 1 \ 1 \ 0]$ . Note that in the  $M_{ge}$  pattern, 1 means that the seed lattice of the  $generator(n, m)$  is filled, otherwise it is not filled. The other two patterns are similar. The first two patterns ( $M_{se}$  and  $M_{ge}$ ) are our primary focus, and the third one serves as a variant to emphasize the potential enhancement effect of local energy clusters (refer to Fig. S1 in our previous work [58]).

The level leg in Fig. 1 demonstrates that several critical states form a subband cluster, influenced by specific parameters such as the  $generator(n, m)$ , the geometrical hi-

erarchy level  $g^*$ , and the dilation patterns represented by matrices  $M_{se}$  and  $M_{ge}$ . This formation is discussed further in Ref. [58]. Moreover, the clustering degree of these levels is quantified using the density of states  $\rho_\sigma(E)$  [74], where variations in the width and height of the peak indicate the presence of quasi-degenerate and degenerate states, respectively. Notably, the *self* pattern exhibits a more pronounced level clustering.

Despite the energy level clustering, each subband possesses a detailed internal structure, particularly noticeable at specific in-band positions, which could be described using multifractal energy spectra [32, 75]. Instead of focusing solely on these spectra, the analysis utilizes  $q$ -weight scaling related to the wave function to examine the spatial differences between any two states. The spatial density of these CSs is illustrated using the scaled state density  $Ar|\psi_{E_n}(i)|^2$ , with the scaling factor  $Ar$  corresponding to the lattice size.

Moreover, it is possibly stressed that a small energy-resolved window  $\delta$  (approximately  $10^{-3}t$ ) is used to depict the states within specific energy clusters accurately. This approach averages all states within the energy range  $E_n \pm \delta/2$ , highlighting the (quasi-)degenerate behavior in specific energy clusters. At the same time, it is used for subdiffusion behavior [76], such as benchmarking the autocorrelation function and mean-square displacement of the critical states in different lattices [77–80]. These tools including the energy-correlation spectra [58] are equivalent in capturing the energy spectra or states in statistical views. Here, we would analyze each state one by one.

The second-order fractal dimension  $\mathcal{D}_2^\psi(\psi_E)$  for all states in two  $SC(4, 2, 3)$  lattices, associated with the *self* and *gene* patterns, typically ranges between 0.6 and 0.9.

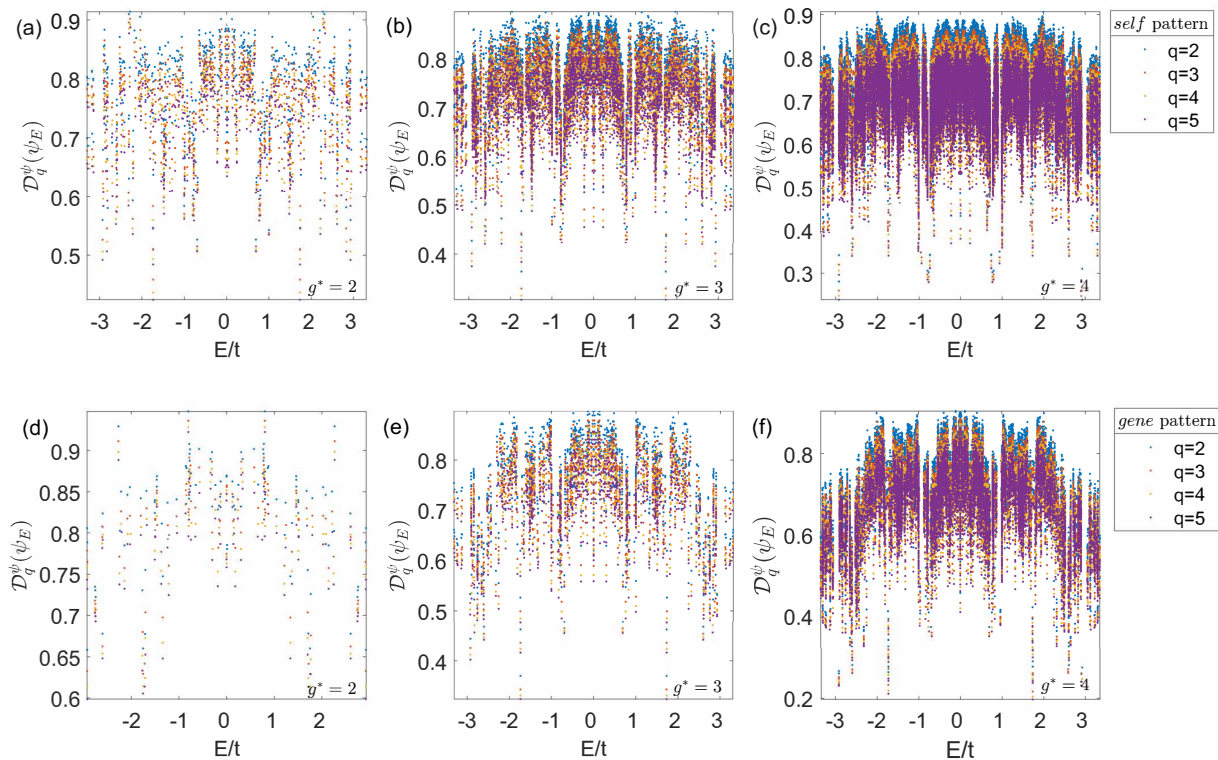


FIG. 2. (Color online) The  $q$ -order fractal dimension  $\mathcal{D}_q^\psi(\psi_E)$  vs critical state  $\psi_E(i)$  at allowed eigenenergy  $E$ . In order to comprise the impact of the dilation pattern, we still use the *generator*(4, 2) as a case. Considering the geometrical hierarchy effect in Ref [58], we modulate  $g^*$  from 2 to 4: the *self* pattern in (a), (b), and (c); and the *gene* pattern in (d), (e), and (f). Here,  $q$  starts from 2 to 5.

The proportion of states within this range is 0.974 and 0.937 for these two patterns, respectively. States outside this range are rare, indicating that the wave functions are predominantly critical. Fig. 1(a) and Fig. 1(b) illustrate four eigenstates with extreme values of  $\mathcal{D}_2^\psi(\psi_E)$ , showcasing the characteristic of partial occupancy in fractals and the spatial overlap between these states.

The eigenstates labeled  $S1$ ,  $S2$ ,  $S3$ , and  $S4$  exhibit a semblance of approximate symmetry, likely resulting from spontaneous symmetry breaking. This characteristic remains consistent across various CSs and in different  $SC(n, m, g^*)$  lattice configurations. However, these symmetrical traits in spatial wavefunction are not universally applicable to most CSs, as evidenced by  $G4$  in Fig 3.

For the *vari* pattern, the fractal dimension  $\mathcal{D}_2^\psi(\psi_E)$  is around 0.3, as shown in Fig. 1(c), which is notably low. This anomaly is primarily attributed to the substantial number of non-connecting site sub-clusters scattered throughout the entire lattice, which are dilated according to the *vari* pattern. This structural feature reduces the connectivity and interference across the lattice, resulting in the significantly lower fractal dimension observed.

To make an analogy, we recall some electrical states in quasicrystals [81]. First, taking the 1D Fibonacci chain [32] case, some electronic states at the band center are self-similar and critical, having  $\psi_m \propto (1/N)^{\alpha_E}$

(where  $\alpha_E$  is the exponent index [47, 82]). Second, the situations become different in Penrose lattice (space dimension  $D = 2$ ), confined states [83, 84] and self-similar state [83] exist in special tiling alignments. Third, in Amman-Kramer lattice ( $D = 3$ ), the electronic states are also critical and have power-law decaying [85].  $\mathcal{D}_q^\psi(\psi_E)$  for electronic states in quasicrystals is less than  $D/2$ , the value of  $D$  depends on the space dimension where the quasicrystals are nested. And  $\mathcal{D}_q^\psi(\psi_E)$  is less than 1 in *Sierpiński* fractals, and it is closer to the fractal dimension  $\mathcal{D}$ . Additionally, the quasicrystals are lacuna-free, however, the fractals have lots of lacuna [86, 87]. Hence the typical power-law character of some critical states is almost absent in fractals.

## B. The multifractality analysis in the $SC(n, m, g^*)$ lattices

For multifractal critical states, we could utilize the state-based fractal dimension  $\mathcal{D}_q^\psi(\psi_E)$  to characterize their distinctive features, notably how the value of  $\mathcal{D}_q^\psi(\psi_E)$  varies with the scaling parameter  $q$  [32, 88–92]. Without other statements throughout the article, the entire fractal lattice (where  $Ar$  denotes the fractal lattice size) is considered, hence  $\Omega = Ar$  is set. Gen-



erally, electronic states exhibit different behaviors when a single electron is situated at various energy levels, resulting in  $\mathcal{D}_q^\psi(\psi_E)$  being dependent on the energy  $E$ , as depicted in Fig. 2. The hole-particle symmetry further makes  $\mathcal{D}_q^\psi(\psi_E)$  symmetric around  $E = 0$  across the entire spectrum of  $\mathcal{D}_q^\psi(\psi_E)$ .

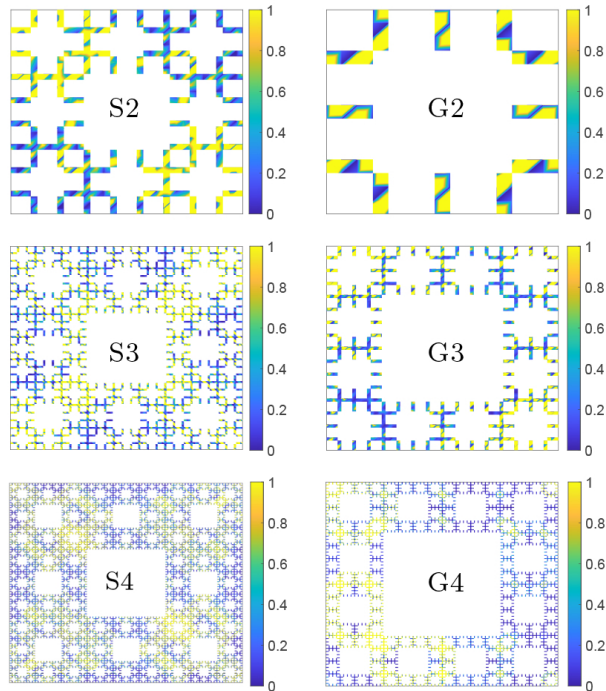


FIG. 3. (Color online) The scaled state density profile  $Ar|\psi_E(i)|^2$  for six center states closest to the band center, are sequentially tagged as S2 in  $SC(4, 2, 2)$  lattice, S3 in  $SC(4, 2, 3)$  lattice, and S4 in  $SC(4, 2, 4)$  lattice for the *self* pattern; and G2 in  $SC(4, 2, 2)$  lattice, G3 in  $SC(4, 2, 3)$  lattice, and G4 in  $SC(4, 2, 4)$  lattice for the *gene* pattern. To visualize these center states vividly, the above six lattices are scaled in the same size. The scaled factor is the lattice size  $Ar$ , and the colorbar range maps from 0 to 1 (In units of  $Ar$ ).

In the following, we would study how these CSs change with the geometrical hierarchy level  $g^*$ , the two dilation types of the *self* and *gene* pattern, and the *generator*( $n, m$ ). First, we assess the influence of the geometric hierarchy level  $g^*$ , which is pivotal for self-similarity objects. In Fig. 2(a), (b), and (c), we select the *generator*(4, 2) as a case. In the *self* pattern, the  $q$ -weighted fractal dimension  $\mathcal{D}_q^\psi(\psi)$  remains between 0.5 and 0.85 when  $g^* = 2$  in Fig. 2(a); when  $g^*$  increases to 3,  $\mathcal{D}_q^\psi(\psi)$  undergoes slight adjustments but generally stays within the same range, as shown in Fig. 2(b). Concurrently, many CSs cluster closely in the energy band and overlap within the spatial lattice, a phenomenon induced by the level attraction effect of  $g^*$ . As  $g^*$  escalates to 4, the maximum value we can simulate, the profiles of  $\mathcal{D}_q^\psi(\psi)$  in Fig. 2(c) resemble those at  $g^* = 3$ .

We turn to the *gene* pattern, when  $g^*$  varies from 2 to 4, the entire span of  $\mathcal{D}_q^\psi(\psi)$  narrows, and the distinct

subclusters become apparent (refer to Fig. 2(d), 2(e), and 2(f)). This effect is presumably due to the strong correlations between the CSs, whose energy levels are closely aligned, possibly leading to the anomalous level-spacing statistic  $P(s)$  [58].

We further fix the value of  $g^*$  to compare the influence of dilation patterns on these critical states. With  $g^* = 2$ , the spectra of  $\mathcal{D}_q^\psi(\psi)$  display identical contours, as seen in Fig 2(a) and Fig 2(d), indicating that the *generator*(4, 2) plays a decisive role in shaping the electronic profile within fractal lattices. This behavior becomes more pronounced when increasing  $g^*$  to 3 (Fig 2(b) and Fig 2(e)) or 4 (Fig 2(c) and Fig 2(f)). It is noteworthy that the overall fluctuation range of  $\mathcal{D}_q^\psi(\psi)$  in the six scenarios is predominantly influenced by the lattice size  $Ar$  of  $SC(4, 2, g^* = 2-4)$ , where  $Ar$  is readily determined by the perimeter-area law [15, 58, 93].

In the six scenarios mentioned above, we further analyze six approximated center-states in the energy band (specifically,  $E \simeq 0$ ), labeled as S2-S4 and G2-G4 in Fig. 3). These multifractal critical states involve wave interference on a size scale relative to the entire lattice. Five of these states (S2-S4 and G2-G3) are nearly symmetrical, which might be attributed to the disrupted translational symmetry and the discrete scaling invariance. Moreover, it is essential to highlight that, due to their unique structure, unlike in *Sierpiński gasket*, the diversity between spatial bulk state and the boundary state in these fractals is challenging, which has been observed by the Hall states [61] in fractal.

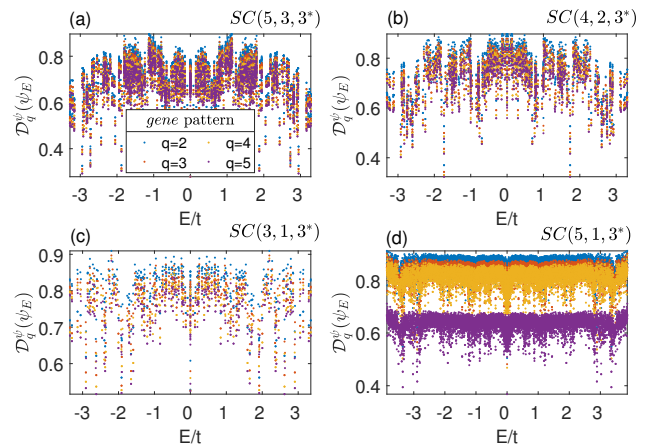


FIG. 4. (Color online)  $\mathcal{D}_q^\psi(\psi_E)$  vs critical state  $\psi_E(i)$  at allowed eigenenergy  $E$  under the *gene* pattern. The impact of the *generator*( $n, m$ ) is comprised by taking (5, 3), (4, 2), (3, 1), and (5, 1) with the unchanged  $g^* = 3$ , in four panels of (a), (b), (c), and (d). Here,  $q$  is still from 2 to 5. Note that the averaged  $\langle \mathcal{D}_2^\psi(\psi) \rangle$  in four cases is 0.7312, 0.7531, 0.8035, 0.8621, respectively.

The *Hausdorff dimension*  $\mathcal{D}$  is essential for fractal objects and affects their quantum transport behaviors [59]. In our study,  $\mathcal{D}_{se}$  is influenced not only by the choice of ( $r, N$ ), but also by the *generator*( $n, m$ ) and geo-

metrical hierarchy level  $g^*$ ;  $\mathcal{D}_{ge}$  is solely determined by its *generator*( $n, m$ ). By applying the perimeter-area law [15, 93] to derive  $\mathcal{D}$ ,  $\mathcal{D}_{se}$  asymptotically follows  $\mathcal{D}_{se} = \lg(N)/\lg(r)$  in the *self* pattern (considering a large value of  $g^*$ ,  $r$  and  $N$  refer in Ref. [58]), and  $\mathcal{D}_{ge} = \lg(n^2 - m^2)/\lg(n)$  in the *gene* pattern [58]. Note that  $\mathcal{D}_{se}$  is only modulated in large fractal lattices, which makes simulation or experimental efforts difficult. We now wish to demonstrate the impact of  $\mathcal{D}_{ge}$ , and  $\mathcal{D}_{se}$  is shown in Appendix A.

$\mathcal{D}_{ge}$  is generally varied by its *generator*( $n, m$ ), making it easier to modulate in the case of small  $g^*$  value. We select the sequence of (5, 3), (4, 2), (3, 1), and (5, 1), resulting in  $\mathcal{D}_{ge}$  gradually increases from 1.7227 and 1.9746. In Fig. 4, we set  $g^* = 3$ , its spectra of  $\mathcal{D}_{ge}$  is significantly influenced by the *generator*( $n, m$ ), as demonstrated in the four cases of (5,3), (4,2), (3,1) and (4,2). And We consider all the CSs, the averaged  $\langle \mathcal{D}_2^\psi(\psi) \rangle$  for four cases is 0.7312, 0.7531, 0.8035, 0.8621, respectively. It is evident the increase of  $\mathcal{D}_{ge}$  causes that the transition from the critical state to the extended state. There is a case in the *SC*(5, 1, 3) lattice, as we discussed in Ref [58], for a *generator*( $n, m$ ) with a large  $n$  and small  $m$ , the expanding lattices under the *gene* pattern can be characterized as the translation-symmetry lattices with certain point-like or cluster-like defects. Consequently, their wave functions are slightly extended, and  $\mathcal{D}_{ge}$  tends towards 1.

#### IV. SUMMARY

In summary, by scaling the inverse participation ratio and visualizing the wavefunction profile, we have analyzed electronic critical states upon fractal *SC*( $n, m, g^*$ ) lattices that are percolated under two typical patterns of the *self* pattern and the *gene* pattern. We have found that the critical states generally exhibit the fragmentation behavior upon fractal *SC*( $n, m, g^*$ ) lattices. Therefore, it causes the electronic states to behave multicritically in fractals with  $\mathcal{D}_q^\psi(\psi_E)$  lessing 1. Note that we ascribed the above confinement effects to the hierarchical properties of fractal structure. It could be observed by the autocorrelation function  $C(t) \sim t^{-\gamma}$  and the mean-square displacement  $d^2(t) \sim t^\delta$ , with the predictions ( $0 < \gamma < 1$  and  $0 < \delta < 1$ ) for these critical states in more giant fractal lattices). For the *gene* pattern and the *self* pattern that we focus on, the fractal dimension  $\mathcal{D}_2^\psi(\psi_E)$  is consistently greater than 0.5, which suggests that there is substantial spatial overlap among these critical states.

Besides, these states have the approximate symmetry when we pinned their energy near 0. As we know, physical states can be classified according to their transport properties. The Periodic Bloch functions describe the conducting states in crystalline systems, and the localized states in insulating systems exhibit exponential decaying. However, when discussing the critical states, the thing gets somewhat tricky. Generally speaking, they

show strong spatial fluctuations at different scales [94], occasionally accompanied by oscillatory behavior, which is evident in *Sierpiński* fractals. We also emphasize that in aperiodic lattices, many mechanisms possibly prevent the wave function from decaying on large scales and not being constant over the entire lattice. There are some cases: i) for flux-threaded Koch fractals, under the action of commutation condition and special magnetic flux,  $\psi(r_i)$  is certainly extended when pinning its eigenvalue in special energy window [17]; ii) for copper-mean chain [25] or period-doubling chain [26], local cluster correlation makes  $\psi(r_i)$  have the similar feature at some energy position, and some critical wave functions tend to expand in 1D Fibonacci chain [29] and Thue-Morse lattice [48] due to short-range atom correlation; iii) both scale invariance and the finite order of ramification cause some states to be somewhat extended in Siperpinski gasket [27, 28].

The interesting thing is that spectra of  $\mathcal{D}_q^\psi(\psi_E)$  are determinedly modulated by the 'seed lattice' of *generator*( $n, m$ ), and slightly changed with the geometrical hierarchy level  $g^*$  and/or the dilation pattern. Additionally, the averaged fractal dimension  $\mathcal{D}_2^\psi(\psi_E)$  would slightly raise with the  $\mathcal{D}_{ge}$ .

Note that comparing the observed properties in irregular objects that whose frontier is fractal-like, including the strong location traits in fractal drum [95, 96], the rich coherence of eigen wavefunction in Koch structure and Koch snowflake [97]. Our work provides some insight about *Sierpiński* lattice. the spectra of energy-level statistics [58] and  $\mathcal{D}_2^\psi(\psi_E)$  could assist the understanding the transport properties [59], optical spectra [98], Hall conductivity [61], even superconductivity [63] in *Sierpiński* lattices. At the same time, our work contributes to further study of disordered-induced localization or even many-body localization from the initial fractal-induced critical phase, and similar studies [71, 99] have been replicated in quasicrystals.

#### V. ACKNOWLEDGMENTS

We thank Dr. Achille Mauri for discussing this work with us. This work was supported by the National Natural Science Foundation of China (Grant No. 12174291), the Natural Science Foundation of Hubei Province, China (2022BAA017, 2023BAA020), and the Core Facility of Wuhan University. Q.Y. acknowledges the China Scholarship Council (CSC) grant by file No. 202006270212 when attending Radboud University in the Netherlands.

#### Appendix A: The spectra of $\mathcal{D}_q^\psi(\psi_E)$ in the *self* pattern

In the main text, our discussion is primarily focused on the *gene* pattern. This pattern is crucial for understanding the behavior of single electron in fractal lattices,

particularly in terms of the fractal dimensions and the localization properties of the wavefunctions.

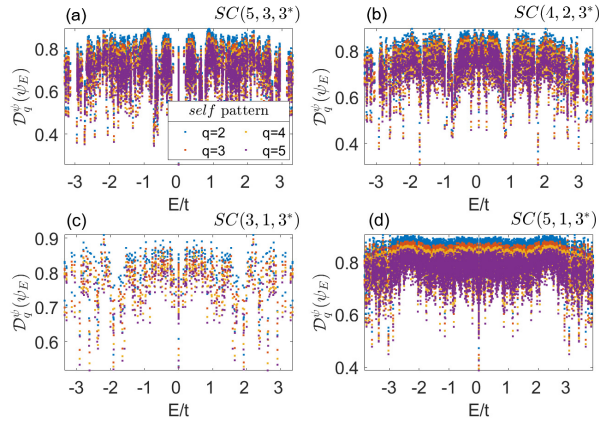


FIG. S1. (Color online) Similar to Fig. 4, the impact of the  $generator(n, m)$  is comprised under the  $self$  pattern. And taking geometrical hierarchy level  $g^* = 3$ , the  $(n, m)$  of  $(5, 3)$ ,  $(4, 2)$ ,  $(3, 1)$ , and  $(5, 1)$  are in (a), (b), (c), and (d), respectively. Here,  $q$  is still from 2 to 5.

To complement this analysis, we have included Fig. S1 with the  $self$  pattern. This figure would illustrate how the spectra of  $\mathcal{D}_q^\psi(\psi_E)$  correlates with the critical states  $\psi_E(i)$  across different configurations. By fixing the geometrical hierarchy level  $g^*$ , we vary the  $generator(n, m)$ , and the overall sketch profile of  $\mathcal{D}_q^\psi(\psi_E)$  is modulated substantially, see Fig. S1(a), (b), (c), (d). Note that the  $\mathcal{D}_q^\psi(\psi_E)$  also reaches 0.9 in Fig. S1(d), which is due to the finite size effect. However,  $\mathcal{D}_q^\psi(\psi_E)$  should decrease when taking the large value of  $g^*$ ; it is beyond the possible simulation ability of our computation station.

## Appendix B: Constructing Sierpiński Carpet $SC(n, m, g^*)$ lattices

First, we need a “seed” lattice (we named it the  $generator(n, m)$ , and  $g^*$  is geometric hierarchy level) and dilation pattern including the  $self$  pattern  $M_{se}$  and the  $gene$  pattern  $M_{ge}$ . Second, we construct the different

types of  $SC(n, m, g^*)$  lattice under the Eq. B1,

$$SC(n, m, g) = M_{se, ge}(g) \otimes generator(n, m), \quad (B1)$$

where  $g$  is hierarchy level, having  $M_{se, ge}(g) \equiv M_{se, ge}(g-1) \otimes M_{se, ge}(1)$ . And  $g$  is distinguished from  $g^*$ , which is discussed in previous work [58]. In Fig. 1,  $SC(4, 2, 3^*)$  lattices are constructed with the  $generator(4, 2)$  under three patterns (the third pattern is the  $vari$  pattern, which is a variation of the  $self$  pattern). Here, we only focus on the first two patterns.

For the  $self$  pattern, comprising the  $SC(n, m, g^* - 1)$  lattice, the perimeter length of the  $SC(n, m, g^*)$  lattice at the  $g^*$ -th iteration increases by  $r$  times and its area increases by  $N$  times. For consistency with Ref [58], supposing  $M_{se} = [1, 1, 1; 1, 0, 1; 1, 1, 1]$  with  $r = 3$  and  $N = 8$ , see Fig. S2(a) and (b). For the  $gene$  pattern, its pattern depends on its “seed” lattice of the  $generator(4, 2)$ , and we have  $M_{ge}(1) = [1, 1, 1, 1; 1, 0, 0, 1; 1, 0, 0, 1; 1, 1, 1, 1]$ , see Fig. S2(c) and (d).

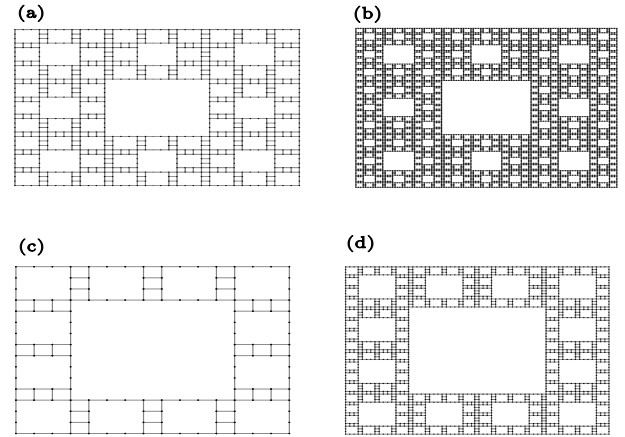


FIG. S2. (Color online) Four  $SC(4, 2, g^*)$  lattices in two dilation pattern. The same “seed” lattice of the  $generator(4, 2)$  is used to construct the  $SC(4, 2, 2)$  (a) and  $SC(4, 2, 3)$  (b) in the  $self$  pattern, and the  $SC(4, 2, 2)$  (c) and  $SC(4, 2, 3)$  (d) in the  $gene$  pattern.

- 
- [1] C. Kittel, *Introduction to solid state physics Eighth edition* (John Wiley & Sons, Inc, 2021).
  - [2] N. Ashcroft and N. D. Mermin, *Solid State Physics* (Saunders College Publishing, 1976).
  - [3] S. V. Vonsovsky and M. I. Katsnelson, *Quantum Solid State Physics* (Springer, 1989).
  - [4] P. Phillips, *Advanced solid state physics* (Cambridge University Press, 2012).
  - [5] M. El-Batanouny, *Advanced Quantum Condensed Matter Physics: One-Body, Many-Body, and Topological Perspectives* (Cambridge University Press, 2020).
  - [6] N. F. Mott and E. A. Davis, *Electronic Processes in Non-Crystalline Materials* (Oxford University Press, 1971).
  - [7] J. M. Ziman, *Models of Disorder* (Cambridge University Press, 1979).
  - [8] I. M. Lifshitz, S. A. Gredeskul, and L. A. Pastur, *Introduction to the Theory of Disordered Systems* (Wiley, 1988).
  - [9] D. Shechtman, I. Blech, D. Gratias, and J. W. Cahn, Metallic phase with long-range orientational order and no translational symmetry, *Phys. Rev. Lett.* **53**, 1951 (1984).



- [10] H. Tsunetsugu, T. Fujiwara, K. Ueda, and T. Tokihiro, Electronic properties of the penrose lattice. i. energy spectrum and wave functions, *Phys. Rev. B* **43**, 8879 (1991).
- [11] H. Tsunetsugu and K. Ueda, Electronic properties of the penrose lattice. ii. conductance at zero temperature, *Phys. Rev. B* **43**, 8892 (1991).
- [12] F. P. M. Beenker, *Algebraic theory of non-periodic tilings of the plane by two simple building blocks: a square and a rhombus* (Eindhoven University of Technology, 1982).
- [13] B. Grünbaum and G. C. Shephard, *Tilings and patterns* (Courier Dover Publications, 1987).
- [14] B. B. Mandelbrot, *The fractal geometry of nature*, Vol. 1 (WH freeman New York, 1982).
- [15] J. Feder, *Fractals* (Springer Science & Business Media, 2013).
- [16] T. Nakayama and K. Yakubo, *Fractal concepts in condensed matter physics*, Vol. 140 (Springer Science & Business Media, 2003).
- [17] S. Biswas and A. Chakrabarti, Complete escape from localization on a hierarchical lattice: A koch fractal with all states extended, *Phys. Rev. B* **108**, 125430 (2023).
- [18] P. W. Anderson, Absence of diffusion in certain random lattices, *Phys. Rev.* **109**, 1492 (1958).
- [19] F. Evers and A. D. Mirlin, Anderson transitions, *Rev. Mod. Phys.* **80**, 1355 (2008).
- [20] E. Domany, S. Alexander, D. Bensimon, and L. P. Kadanoff, Solutions to the schrödinger equation on some fractal lattices, *Phys. Rev. B* **28**, 3110 (1983).
- [21] Q. Niu and F. Nori, Renormalization-group study of one-dimensional quasiperiodic systems, *Phys. Rev. Lett.* **57**, 2057 (1986).
- [22] A. Chakrabarti and S. N. Karmakar, Renormalization-group method for exact green's functions of self-similar lattices: Application to generalized fibonacci chains, *Phys. Rev. B* **44**, 896 (1991).
- [23] X. H. Yan, J. X. Zhong, J. R. Yan, and J. Q. You, Renormalization group of generalized fibonacci lattices, *Phys. Rev. B* **46**, 6071 (1992).
- [24] J. Q. You, J. R. Yan, J. X. Zhong, and X. H. Yan, Local electronic properties of two-dimensional penrose tilings: A renormalization-group approach, *Phys. Rev. B* **45**, 7690 (1992).
- [25] S. Sil, S. N. Karmakar, R. K. Moitra, and A. Chakrabarti, Extended states in one-dimensional lattices: Application to the quasiperiodic copper-mean chain, *Phys. Rev. B* **48**, 4192 (1993).
- [26] A. Chakrabarti, S. N. Karmakar, and R. K. Moitra, Renormalization-group analysis of extended electronic states in one-dimensional quasiperiodic lattices, *Phys. Rev. B* **50**, 13276 (1994).
- [27] A. Chakrabarti, Exact results for infinite and finite sierpinski gasket fractals: extended electron states and transmission properties, *Journal of Physics: Condensed Matter* **8**, 10951 (1996).
- [28] S. Biswas and A. Chakrabarti, Designer quantum states on a fractal substrate: Compact localization, flat bands and the edge modes, *Physica E: Low-dimensional Systems and Nanostructures* **153**, 115762 (2023).
- [29] E. Maciá and F. Domínguez-Adame, Physical nature of critical wave functions in fibonacci systems, *Phys. Rev. Lett.* **76**, 2957 (1996).
- [30] A. Eilmes, R. Römer, and M. Schreiber, The two-dimensional anderson model of localization with random hopping, *The European Physical Journal B* **1**, 29 (1998).
- [31] Z. M. Stadnik, *Physical Properties of Quasicrystals* (Springer, 1999).
- [32] A. Jagannathan, The fibonacci quasicrystal: Case study of hidden dimensions and multifractality, *Rev. Mod. Phys.* **93**, 045001 (2021).
- [33] F. J. Dyson, Statistical theory of the energy levels of complex systems. i, *Journal of Mathematical Physics* **3**, 140 (1962).
- [34] M. L. Mehta, *Random matrices* (Academic, New York, 1991).
- [35] K. Efetov, *Supersymmetry in disorder and chaos* (Cambridge university press, 1999).
- [36] R. Cafiero, A. Gabrielli, M. Marsili, M. A. Muñoz, and L. Pietronero, Generalized dielectric breakdown model, *Phys. Rev. B* **60**, 786 (1999).
- [37] T. Nakayama, K. Yakubo, and R. L. Orbach, Dynamical properties of fractal networks: Scaling, numerical simulations, and physical realizations, *Rev. Mod. Phys.* **66**, 381 (1994).
- [38] A. Mirlin, Statistics of energy levels and eigenfunctions in disordered systems, *Physics Reports* **326**, 259 (2000).
- [39] I. K. Zharekeshev and B. Kramer, Scaling of level statistics at the disorder-induced metal-insulator transition, *Phys. Rev. B* **51**, 17239 (1995).
- [40] K. R. Amin, R. Nagarajan, R. Pandit, and A. Bid, Multifractal conductance fluctuations in high-mobility graphene in the integer quantum hall regime, *Phys. Rev. Lett.* **129**, 186802 (2022).
- [41] A. L. R. Barbosa, T. H. V. de Lima, I. R. R. González, N. L. Pessoa, A. M. S. Macêdo, and G. L. Vasconcelos, Turbulence hierarchy and multifractality in the integer quantum hall transition, *Phys. Rev. Lett.* **128**, 236803 (2022).
- [42] X. Yang, W. Zhou, Q. Yao, P. Lv, Y. Wang, and S. Yuan, Electronic properties and quantum transport in functionalized graphene sierpinski-carpet fractals, *Phys. Rev. B* **105**, 205433 (2022).
- [43] M. Kohmoto and B. Sutherland, Electronic states on a penrose lattice, *Phys. Rev. Lett.* **56**, 2740 (1986).
- [44] N. Macé, A. Jagannathan, P. Kalugin, R. Mosseri, and F. Piéchon, Critical eigenstates and their properties in one- and two-dimensional quasicrystals, *Phys. Rev. B* **96**, 045138 (2017).
- [45] W. Zhou and S. Yuan, A time-dependent random state approach for large-scale density functional calculations, *Chin. Phys. Lett.* **40**, 027101 (2023).
- [46] M. Quilichini, Phonon excitations in quasicrystals, *Rev. Mod. Phys.* **69**, 277 (1997).
- [47] M. Kohmoto, B. Sutherland, and C. Tang, Critical wave functions and a cantor-set spectrum of a one-dimensional quasicrystal model, *Phys. Rev. B* **35**, 1020 (1987).
- [48] A. Chakrabarti, S. N. Karmakar, and R. K. Moitra, Role of a new type of correlated disorder in extended electronic states in the thue-morse lattice, *Phys. Rev. Lett.* **74**, 1403 (1995).
- [49] B. Sutherland, Self-similar ground-state wave function for electrons on a two-dimensional penrose lattice, *Phys. Rev. B* **34**, 3904 (1986).
- [50] G. R. Newkome, P. Wang, C. N. Moorefield, T. J. Cho, P. P. Mohapatra, S. Li, S.-H. Hwang, O. Lukyanova, L. Echegoyen, J. A. Palagallo, V. Iancu, and S.-W. Hla, Nanoassembly of a fractal polymer: A molecular "sierpinski hexagonal gasket", *Science* **312**, 1782 (2006).



- [51] J. A. Fan, W.-H. Yeo, Y. Su, Y. Hattori, W. Lee, S.-Y. Jung, Y. Zhang, Z. Liu, H. Cheng, L. Falgout, M. Bajema, T. Coleman, D. Gregoire, R. J. Larsen, Y. Huang, and J. A. Rogers, Fractal design concepts for stretchable electronics, *Nat. Commun.* **5**, 3266 (2014).
- [52] J. Shang, Y. Wang, M. Chen, J. Dai, X. Zhou, J. Kuttner, G. Hilt, X. Shao, J. M. Gottfried, and K. Wu, Assembling molecular sierpiński triangle fractals, *Nat. Chem.* **7**, 389 (2015).
- [53] C. Liu, Y. Zhou, G. Wang, Y. Yin, C. Li, H. Huang, D. Guan, Y. Li, S. Wang, H. Zheng, C. Liu, Y. Han, J. W. Evans, F. Liu, and J. Jia, Sierpiński structure and electronic topology in bi thin films on insb(111)b surfaces, *Phys. Rev. Lett.* **126**, 176102 (2021).
- [54] Z. Yang, E. Lustig, Y. Lumer, and M. Segev, Photonic floquet topological insulators in a fractal lattice, *Light Sci. Appl.* **9**, 128 (2020).
- [55] L. Song, H. Yang, Y. Cao, and P. Yan, Realization of the square-root higher-order topological insulator in electric circuits, *Nano Lett.* **20**, 7566 (2020).
- [56] J. Li, Y. Sun, Q. Mo, Z. Ruan, and Z. Yang, Fractality-induced topological phase squeezing and devil's staircase, *Phys. Rev. Res.* **5**, 023189 (2023).
- [57] S. N. Kempkes, M. R. Slot, S. E. Freney, S. J. M. Zevenhuizen, D. Vanmaekelbergh, I. Swart, and C. M. Smith, Design and characterization of electrons in a fractal geometry, *Nature Phys.* **15**, 127 (2018).
- [58] Q. Yao, X. Yang, A. A. Iliasov, M. I. Katsnelson, and S. Yuan, Energy-level statistics in planar fractal tight-binding models, *Phys. Rev. B* **107**, 115424 (2023).
- [59] E. van Veen, S. Yuan, M. I. Katsnelson, M. Polini, and A. Tomadin, Quantum transport in sierpinski carpets, *Phys. Rev. B* **93**, 115428 (2016).
- [60] T. Westerhout, E. van Veen, M. I. Katsnelson, and S. Yuan, Plasmon confinement in fractal quantum systems, *Phys. Rev. B* **97**, 205434 (2018).
- [61] A. A. Iliasov, M. I. Katsnelson, and S. Yuan, Hall conductivity of a sierpiński carpet, *Phys. Rev. B* **101**, 045413 (2020).
- [62] The fractals-induced critical phase could be driven to the localization phase by increasing the disorder strength, and one observe the energy level-correlation spectra gradually transitioning from the Wigner-like distribution to the Poisson distribution, and multifractal critical states trend to the localized states.
- [63] A. A. Iliasov, M. I. Katsnelson, and A. A. Bagrov, Strong enhancement of superconductivity on finitely ramified fractal lattices (2024), [arXiv:2310.11497 \[cond-mat.supr-con\]](https://arxiv.org/abs/2310.11497).
- [64] P. G. Harper, Single band motion of conduction electrons in a uniform magnetic field, *Proc. Phys. Soc. Sect. A* **68**, 874 (1955).
- [65] S. Aubry and G. André, Analyticity breaking and anderson localization in incommensurate lattices, *Ann. Israel Phys. Soc* **3**, 18 (1980).
- [66] P. G. Harper, The general motion of conduction electrons in a uniform magnetic field, with application to the diamagnetism of metals, *Proc. Phys. Soc. Sect. A* **68**, 879 (1955).
- [67] C. M. Soukoulis and E. N. Economou, Fractal character of eigenstates in disordered systems, *Phys. Rev. Lett.* **52**, 565 (1984).
- [68] P. de Vries, H. De Raedt, and A. Lagendijk, Localization of waves in fractals: Spatial behavior, *Phys. Rev. Lett.* **62**, 2515 (1989).
- [69] I. Varga, E. Hofstetter, and J. Pipek, One-parameter super-scaling at the metal-insulator transition in three dimensions, *Phys. Rev. Lett.* **82**, 4683 (1999).
- [70] J. Pipek and I. Varga, Universal classification scheme for the spatial-localization properties of one-particle states in finite, d-dimensional systems, *Phys. Rev. A* **46**, 3148 (1992).
- [71] Y. Wang, X. Xia, L. Zhang, H. Yao, S. Chen, J. You, Q. Zhou, and X.-J. Liu, One-dimensional quasiperiodic mosaic lattice with exact mobility edges, *Phys. Rev. Lett.* **125**, 196604 (2020).
- [72] M. Janssen, Statistics and scaling in disordered mesoscopic electron systems, *Phys. Rep.* **295**, 1 (1998).
- [73] M. Janssen, Multifractal analysis of broadly-distributed observables at criticality, *International Journal of Modern Physics B* **08**, 943 (1994).
- [74] The stair-like DoS,  $\rho(E) = 1/Ar \sum_{k=1}^{Ar} \delta(E - E_k)$ , would be blurred with a smooth function  $g_\sigma(t)$ . When we regularize the Dirac function  $\delta(t)$  by Gaussian or Lorentz function  $g_\sigma(t)$ ,  $\rho_\sigma(E)$  usually has a smoother curve.
- [75] I. Guarneri, On an estimate concerning quantum diffusion in the presence of a fractal spectrum, *Europhysics Letters (EPL)* **21**, 729 (1993).
- [76] G. De Tomasi, S. Bera, A. Scardicchio, and I. M. Khaymovich, Subdiffusion in the anderson model on the random regular graph, *Phys. Rev. B* **101**, 100201 (2020).
- [77] B. O'Shaughnessy and I. Procaccia, Diffusion on fractals, *Phys. Rev. A* **32**, 3073 (1985).
- [78] L. Guidoni, B. Dépret, A. di Stefano, and P. Verkerk, Atomic diffusion in an optical quasicrystal with five-fold symmetry, *Phys. Rev. A* **60**, R4233 (1999).
- [79] L. Basnarkov and V. Urumov, Diffusion on archimedean lattices, *Phys. Rev. E* **73**, 046116 (2006).
- [80] M. A. Di Muro and M. Hoyuelos, Diffusion on a lattice: Transition rates, interactions, and memory effects, *Phys. Rev. E* **106**, 014139 (2022).
- [81] Z. M. Stadnik, *Physical properties of quasicrystals*, Vol. 126 (Springer Science & Business Media, 2012).
- [82] T. Fujiwara, M. Kohmoto, and T. Tokihiro, Multifractal wave functions on a fibonacci lattice, *Phys. Rev. B* **40**, 7413 (1989).
- [83] T. Tokihiro, T. Fujiwara, and M. Arai, Exact eigenstates on a two-dimensional penrose lattice and their fractal dimensions, *Phys. Rev. B* **38**, 5981 (1988).
- [84] T. Fujiwara, Electronic structure in the al-mn alloy crystalline analog of quasicrystals, *Phys. Rev. B* **40**, 942 (1989).
- [85] T. Rieth and M. Schreiber, Numerical investigation of electronic wave functions in quasiperiodic lattices, *Journal of Physics: Condensed Matter* **10**, 783 (1998).
- [86] Y. Gefen, Y. Meir, B. B. Mandelbrot, and A. Aharony, Geometric implementation of hypercubic lattices with noninteger dimensionality by use of low lacunarity fractal lattices, *Phys. Rev. Lett.* **50**, 145 (1983).
- [87] B. Lin, Classification and universal properties of sierpinski carpets, *Journal of Physics A: Mathematical and General* **20**, L163 (1987).
- [88] Y. Hatsugai and M. Kohmoto, Energy spectrum and the quantum hall effect on the square lattice with next-nearest-neighbor hopping, *Phys. Rev. B* **42**, 8282 (1990).
- [89] X. Cai, L.-J. Lang, S. Chen, and Y. Wang, Topological superconductor to anderson localization transition

- in one-dimensional incommensurate lattices, *Phys. Rev. Lett.* **110**, 176403 (2013).
- [90] F. Liu, S. Ghosh, and Y. D. Chong, Localization and adiabatic pumping in a generalized aubry-andré-harper model, *Phys. Rev. B* **91**, 014108 (2015).
- [91] Y. Wang, L. Zhang, S. Niu, D. Yu, and X.-J. Liu, Realization and detection of nonergodic critical phases in an optical raman lattice, *Phys. Rev. Lett.* **125**, 073204 (2020).
- [92] T. Xiao, D. Xie, Z. Dong, T. Chen, W. Yi, and B. Yan, Observation of topological phase with critical localization in a quasi-periodic lattice, *Science Bulletin* **66**, 2175 (2021).
- [93] B. Mandelbrot, *Fractals* (Freeman San Francisco, 1977).
- [94] É. Brézin, V. Kazakov, D. Serban, P. Wiegmann, and A. Zabrodin, *Applications of random matrices in physics*, Vol. 221 (Springer Science & Business Media, 2006).
- [95] C. Even, S. Russ, V. Repain, P. Pieranski, and B. Sapoval, Localizations in fractal drums: An experimental study, *Phys. Rev. Lett.* **83**, 726 (1999).
- [96] S. Homolya, C. F. Osborne, and I. D. Svalbe, Density of states for vibrations of fractal drums, *Phys. Rev. E* **67**, 026211 (2003).
- [97] A. Adrover and F. Garofalo, Scaling of the density of state of the weighted laplacian in the presence of fractal boundaries, *Phys. Rev. E* **81**, 027202 (2010).
- [98] E. van Veen, A. Tomadin, M. Polini, M. I. Katsnelson, and S. Yuan, Optical conductivity of a quantum electron gas in a sierpinski carpet, *Phys. Rev. B* **96**, 235438 (2017).
- [99] X.-C. Zhou, Y. Wang, T.-F. J. Poon, Q. Zhou, and X.-J. Liu, Exact new mobility edges between critical and localized states, *Phys. Rev. Lett.* **131**, 176401 (2023).